2023 45th Annual International Conference of the IEEE Engineering in Medicine & Biology Society (EMBC) | 979-8-3503-2447-1/23/$31.00 ©2023 IEEE | DOI: 10.1109/EMBC40787.2023.10340768

A Secure Vitals Monitoring Point-of-Care Device

Emily Oliver[1], Rongting Yue[2*] and Abhishek Dutta[2]

***Abstract*— Point-of-care (POC) devices continuously monitor vital signs and provide health suggestions to users. However, the devices are not affordable to everyone due to their cost. Here, we design a POC device that can continuously estimate vital signs using fewer sensors and lower costs. We do so by measuring photoplethysmogram signals and temperature and then estimating the heart rate, blood oxygen saturation, respiration rate, and blood pressure. For keeping the vital data secure, an auto-encoder and a convolutional neural network were also used for encryption and abnormality detection, respectively. Tests on the hardware showed the design accurately obtained users' vitals. The proposed design is expected to be generalized to obtain other vitals and fabricated at a low cost, making it affordable to all people.**

I. Introduction

Point-of-care (POC) devices continuously help users monitor their vitals and provide them with health recommendations, while the requirement of medical personnel for professional medical equipment as well as their invasive techniques hinder people from accessing medical care easily [1]. The commonly tracked vitals include heart rate (HR), body temperature, electrocardiogram (ECG) readings, blood pressure (BP), respiration rate, blood oxygen saturation, blood glucose, skin perspiration, capnography, and motion [2]. Wearable POC devices, such as the Apple Watch, can measure a subset of the vitals and they are smaller, more comfortable devices that can be used in users' everyday life [3]. However, these devices are not affordable to all people, especially for users in developing countries that lack healthcare services. Meanwhile, the lower cost usually corresponds to fewer sensors or less measured vitals, resulting in inaccurate or inadequate data on users' health conditions.

Wearable Internet of Things (IoT) medical devices allow patients to continuously monitor their health at home, which would help reduce medical costs [4]. This is done by connecting the devices to the cloud, such that the vitals collected by sensors can be sent to a server for processing. However, the transmission of big medical data is time-consuming for cloud-based systems, which makes it not beneficial for emergency situations. Deep learning (DL) utilizes deep neural network structure to mine useful and representative information from big data, such that data volume can be heavily reduced. In wearable medical devices, DL can be used to either identify abnormal data or make predictions about diseases [5]. For example, in a Vital-ECG device, features extracted from the ECG and pulse oximetry signals help classify bradycardia and tachycardia [6]. The security and privacy of the devices must also be ensured to protect the medical data from being changed or hacked because of the IoT and cloud-based platforms. Encryption and fog computing can be used to help combat issues, specifically confidentiality and integrity, but these techniques can be complex and difficult to maintain as they are often used with big medical data [7]. Deep learning techniques efficiently extract features from big medical data, which can contribute to security issues. For example, the low-dimensional features in Autoencoders can help classify malware and identify attacks [8].

In this study, a wearable POC device that is affordable, miniaturized, connected and secure was designed, and its block diagram is shown in Figure 1. The device measured temperature and collects the photoplethysmogram (PPG) signal of the user, and then estimated HR, blood oxygen saturation, blood pressure, and respiration rate accordingly. The estimation methods were tested with online datasets and used on human subjects. An autoencoder for encryption and a neural network for abnormality detection were used for security measures. A prototype of this wrist-worn device was implemented in a preliminary Printed Circuit Board (PCB). In future work, a disease prediction algorithm and a treatment control system could be implemented.

II. Materials and Methods

The vital measurements include PPG signals and temperature. The blood pressure, respiration rate, HR, and blood oxygen are estimated based on the measured vitals. An autoencoder is used to obtain extracted features for security.

A. Data Collection

A PPG sensor made up of a light source and a photodetector is used to detect users' HRs. The ratio of light absorbed to light reflected back to the photodetector creates the PPG waveform and allows HR to be calculated [9]. Temperature is measured using an analog temperature sensor with voltage readings with the sensor resolution of 10 $mV/^{\circ}C$ and 12-bit analog-to-digital converter, such that the resolution would be approximately 0.08°C per bit.

B. Vital Estimation

a) Blood Pressure: Blood pressure (BP) is estimated using a combination of HR and normalized pulse volume (mNVP) (i.e., the amplitude of the wave from minimum to

[1]E. Oliver is with the Department of Biomedical Engineering, University of Connecticut, Storrs, CT, 06269, United States

[2]R. Yue and A. Dutta are with the Department of Electrical and Computer Engineering, University of Connecticut, Storrs, CT, 06269, United States

*E-mail for correspondence: rongting.yue@uconn.edu

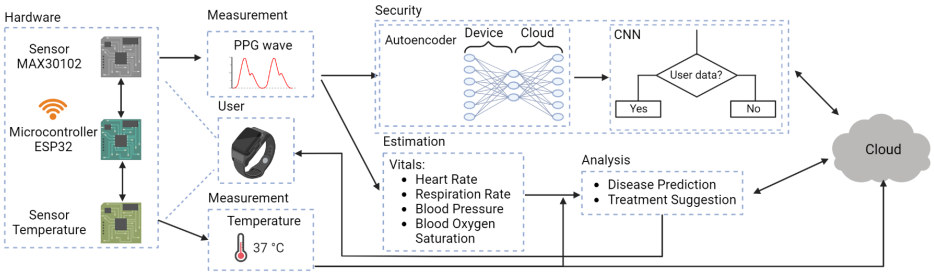

Fig. 1: A block diagram of the designed wearable POC device. Sensors on the device collect PPG signals and temperatures from users. The data is used for secure vitals monitoring using an autoencoder and a series of estimators.

maximum divided by the direct current (DC) value of the signal) and then calculated as [10]:

$$lnBP = (a * \ln HR) + (b * \ln mNVP) + c \tag{1}$$

where a, b, and c are constants determined using linear regression. We use the data set [11] that contains a PPG and blood pressure signal with a sampling rate of 125 Hz. $mNPV$ is calculated every two seconds to find both the AC and DC components of the PPG wave [12].

Respiration Rate: The respiration rate is estimated (as in Equation (2) [13]) from a PPG signal using pulse width variability (PWV) that helps eliminate the problem of motion artifacts.

$$d^u_{PWV}(n) = \sum_i \frac{1}{f^P_s}(n_{E_i} - n_{O_i})\delta(n - n_{A_i}) \tag{2}$$

where n is the time index, f^P_s is the sampling rate, n_{O_i} and n_{E_i} are the moments of the i-th beginning and end of the wave, and n_{A_i} is the moment of the i-th systolic peaks within the signal. Two conditions must be met to differentiate a systolic and diastolic peak in a PPG wave: 1) each maximum must be followed by a minimum, and 2) a threshold based on the user's average heart rate is used to prevent the occurrence of two peaks, which is updated if the heart rate fluctuates. If both conditions are met, the peak is considered systolic. If there is more than one width found within one second, the pulse width variability values are averaged together.

Heart Rate: HR is calculated every two seconds based on PPG signals obtained from sensors using a peak detection: $HR = \frac{60}{t_{pulse}}$, where t_{pulse} is the time between two systolic peaks [12]. Two conditions are set to differentiate a systolic and diastolic peak in a PPG wave: (1) every maximum needs to be followed by a minimum and vice versa; (2) there is a threshold in which two peaks cannot occur, and the threshold is set by the user's average HR and it is updated if the HR fluctuates. Once both conditions are satisfied, a peak is registered as systolic to calculate HR. The Pulse Transit Time PPG Dataset (version 1.1.0) with a sampling rate of 125 Hz is used for tests. Two systolic peaks are considered within a window of two-second (i.e., the sampling rate of 250 Hz). To account for more than two peaks being in the window, all calculations are averaged over the course of two seconds.

Blood Oxygen Saturation: A PPG sensor (typically placed on the finger) measures the amount of light absorbed from both arterial and venous blood using a probe with light-emitting diodes and a photodetector. PPG signals help determine blood oxygen saturation SpO_2, which is approximated using a linear regression model $SpO_2 = a_0 + b_0 * R$, where a_0 and b_0 are coefficients, and R is the ratio of the AC over DC component for red and infrared light on the sensor, as shown in Equation (3) [12]. The test dataset is the same as in HR; however, only the initial and final blood oxygen saturation values are provided. Therefore, the blood oxygen saturation is estimated for the first and last two seconds of the dataset, which are approximately 96.64% and 96.31%, respectively, and compared to the recorded measurement, which are 95% and 98%, respectively.

$$R = \frac{AC_{red}/DC_{red}}{AC_{ir}/DC_{ir}} \tag{3}$$

C. Deep Learning for Device Security

The POC device encrypts the data and identifies if the data has been altered for security issues. An autoencoder is used to transform the PPG data into an unrecognizable low-dimensional space using an encoding scheme on the device, so that attackers wouldn't get useful information (e.g., time of the signal) without knowing the decoder, even if they obtain access to the device or cloud. A decoder located on the cloud is used to reconstruct the original PPG signal. Leaky ReLu activation function $R_L(z) = max(0.01z, z)$ is used to help combat dying neurons, where z is the latent features. Dropout regularization is used to help reduce overfitting. The encoder takes 125 input nodes with 4 fully connected hidden layers that contain 100, 50, 25, and 5 nodes, respectively. Five features from the output of the encoder are regarded as encrypted PPG signals. The decoder is symmetric to the encoder. The mean squared error $MSE = \frac{1}{n}\sum_{i=1}^{n}(Y_i - \hat{Y}_i)^2$ is chosen as the cost function, where n is the number of data points, and $\hat{Y}_i$ is the predicted magnitude of the reconstructed PPG wave at the $i-$th sampling point, and Y_i is the measured magnitude of the original wave.

The convolutional neural network is applied to the decoded PPG waves to detect if the data is altered. A 125-dimensional decrypted PPG wave is input to a 1D convolutional layer with 32 kernels and a ReLu activation function. An average pooling layer is used with a patch size of two. The latent features are flattened for the following dense layer with 16 nodes with a ReLu activation function $R(z) = max(0, z)$. The last layer is a dense layer with a single output node

and the Sigmoid activation function $S(z) = \frac{1}{1+e^{-z}}$. In this case, a value close to 1 indicates a strong probability that the signal is a PPG wave, while a value close to 0 strongly indicates that it is not a PPG signal. To train this classifier, an equal number of PPG waves and the other waves are used. Here we use the PPG waves and the physiological signals of respiration (or impedance respiratory signals) from the dataset [14]. The binary cross entropy is used as the cost function as shown in Equation (4).

$$H_p = -\frac{1}{N}\sum_{i=1}^{N}[y_i \cdot log(p(y_i)) + (1-y_i) \cdot log(1-p(y_i))] \quad (4)$$

where N is the number of waves, and y_i is the label of 1 or 0 that indicates the signal is a PPG wave or not, with the corresponding probability $p(y_i)$.

D. Hardware

The design of the proposed POC device uses the Heltec WiFi Kit 32 with the microcontroller module ESP32 because of its low cost, low power consumption, and compatibility with IoT applications (e.g., WiFi and Bluetooth) and "micropython" (TensorFlow). The low-power biometric sensor MAX30102, which has a wavelength of 660nm for the red light and 880nm for the IR light, is selected for detecting HR and blood oxygen levels. This sensor is small enough to be mounted on a wearable device. The temperature sensor LMT86LMP is used, whose operating range is from -50 to 150 $^{\circ}C$ with an average error of 0.4 $^{\circ}C$.

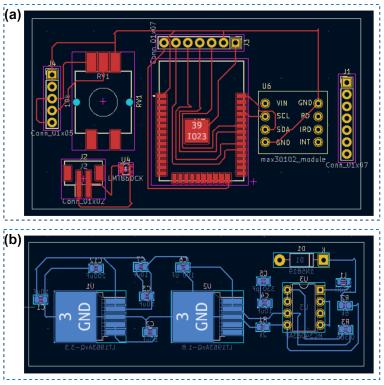

Fig. 2: (a) One side of the printed circuit board; it will rest against the user's skin. (b) The other side of the PCB, is mainly made up of voltage regulators.

These sensors and modules are integrated into a printed circuit board (PCB), which will then be inserted into a strap so it can be worn on the wrist. The design is tested on breadboards for validity. Data and commands are transmitted between the microcontroller and sensors using $I2C$ serial communication. A rechargeable 3.7 V Lithium-Ion Polymer battery is used in the circuit. Two voltage regulators are used to generate 1.8 volts and 3.3 volts output, to power the MAX30102 sensor, the temperature, and the ESP32 chip.

Data are read from Arduino IDE and the built-in screen on Heltec Wifi Kit 32 during the tests. A separate LCD screen can be added in the future PCB to visualize the estimated vitals, and its connector is reserved on the board. A voltage booster using an MC34063 regulator is used to power the modules (e.g., the LCD screen) that generally require 5 V to operate. The designed circuit board is double-sided, with the MAX30102 sensor and the analog temperature sensor facing the skin to record accurate readings, as shown in Figure 2 (a). The other side of the PCB, as shown in Figure 2 (b), contains the necessary components to power the device.

III. Results

Now that a framework has been established for a wearable POC device. Each of the vital estimation methods was tested on human subjects with the sensors placed on a breadboard connected to the Heltec Wifi Kit 32.

A. Vital Estimation Evaluation

a) Heart Rate: HR trials were done on two different human subjects, three times, for thirty seconds each. Subjects placed their finger on the MAX30102 sensor for thirty seconds, where HR was calculated every three seconds. Immediately after this, the subject took their pulse for thirty seconds on their wrist, and doubled it to find their HR. The comparison between the recorded and estimated average HR is shown in Figure 3 (a), where the estimated values were extremely close to the actual, with an average percent error of less than 1%.

b) Blood Oxygen Saturation, Blood Pressure and Respiration Rate: Blood oxygen saturation and blood pressure trials were run with two subjects and taking measurements three times for thirty seconds each. The reading from the MAX30102 sensor was calculated every three seconds, and then averaged for a final reading after thirty seconds. The estimated values were compared to that measured using the device "MorePro V19 Health Tracker", which were taken at the same time as the sensor reading, e.g., after thirty seconds reported the systolic and diastolic blood pressure. For the estimated blood oxygen saturation, the average percent errors were 2.45% and 2.44% for subjects 1 and 2, respectively. For the blood pressures, data from six trials were used to calibrate the parameters in Equation (1). The estimated values and the measured values were almost identical, as shown in Figure 3 (d). The constants [a, b, c] were calculated to be [0.0496, -0.0091, 4.2661], [0.0491, -0.0079, 4.6388] and [0.0490, -0.0102, 4.0150] for mean arterial blood pressure, systolic blood pressure and diastolic blood pressure, respectively. The average percent errors were less than 3.5% when comparing the estimated to measured values every two seconds. The respiration rate was tested on two different subjects using the MAX30102 sensor. Each subject did this three times while breathing normally and counting their breaths. The window lengths of 30, 40, and 60 seconds are tested, with the window sliding by 1 second and then recalculating the respiration rate. The 60-second window produced the best results, with an average percent error of 7.34%, and as seen in Figure 3 (b). The estimated respiration rate was then compared to the number of counted breaths, as shown in Figure 3 (c).

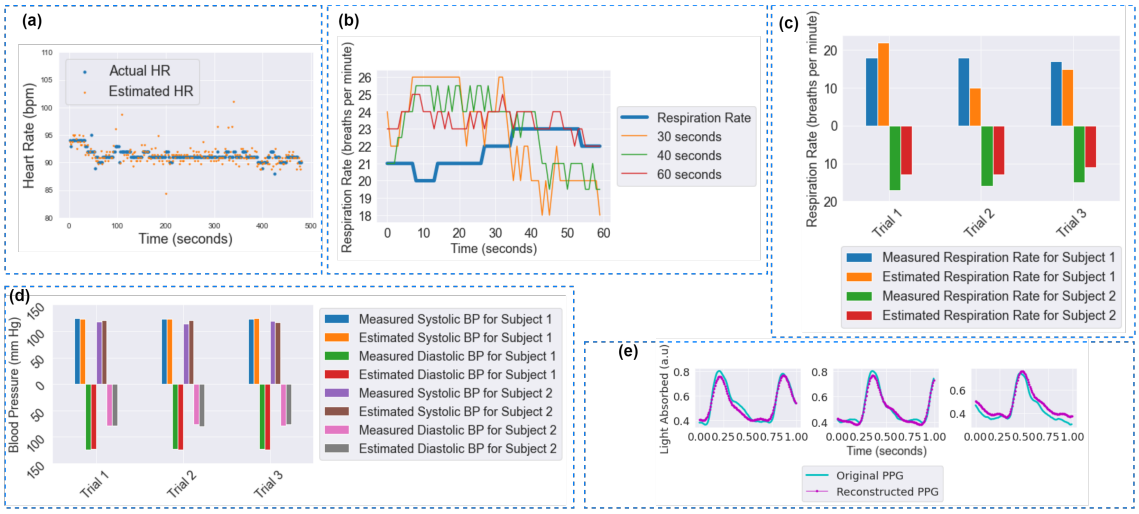

Fig. 3: (a) Estimated versus actual HR for the Pulse Transit Time PPG Dataset, from subject 1 while sitting. (b) The impact of window sizes on the accuracy of the estimated respiration rate. The plot shows the actual and estimated respiration rate of different window sizes. (c) The comparison of estimated versus actual respiration rates for two subjects. (d) The comparison of estimated versus actual systolic and diastolic blood pressure. (e) A comparison between the original PPG signal and the reconstructed signal by autoencoder.

B. System Security

The autoencoder was trained on 40 epochs with a batch size of 100. After 15 epochs, the MSE for this autoencoder was less than 0.004 for training data and less than 0.003 for validation data. The reconstructed PPG was close to the original PPG as shown in Figure 3 (e). Evaluation of the classifier was based on the ratio of the total of true positives (50.06%) and true negatives (49.78%) over the total number of predictions. The false positive and false negative were 0.03% and 0.13%, respectively. The classifier for system security had an accuracy of 99.85%, which demonstrates that the neural network was correctly identifying if the signal was a PPG wave or not. Meanwhile, the encoder encrypted the PPG signal (i.e., the 5 features) to low-dimensional latent space that is not meaningful or interpretable, which indicates the success of encryption.

IV. Conclusions

An affordable wearable POC device that can securely monitor vitals is developed and validated. The device measures PPG signals and temperature, and it estimates the other vitals, including the HR, blood oxygen saturation, blood pressure, and respiration rate. Low errors of the estimated vitals compared to measurements validate the accuracy of the monitoring device designed. Moreover, data is encrypted using an autoencoder to secure the device.

Acknowledgements

We acknowledge the support from the UConn School of Engineering for the research, authorship, and publication of this article.

References

[1] R. Burger and C. Christian, "Access to health care in post-apartheid south africa: availability, affordability, acceptability," *Health Economics, Policy and Law*, vol. 15, no. 1, pp. 43–55, 2020.

[2] D. Dias and J. Paulo Silva Cunha, "Wearable health devices—vital sign monitoring, systems and technologies," *Sensors*, vol. 18, no. 8, p. 2414, 2018.

[3] T. Yilmaz, R. Foster, and Y. Hao, "Detecting vital signs with wearable wireless sensors," *Sensors*, vol. 10, no. 12, pp. 10 837–10 862, 2010.

[4] C. M. Mohammed and S. Askar, "Machine learning for iot healthcare applications: A review," *International Journal of Science and Business*, vol. 5, no. 3, pp. 42–51, 2021.

[5] C. J. Goergen, M. J. Tweardy, S. R. Steinhubl, S. W. Wegerich, K. Singh, R. J. Mieloszyk, and J. Dunn, "Detection and monitoring of viral infections via wearable devices and biometric data," *Annual review of biomedical engineering*, vol. 24, 2021.

[6] V. Randazzo, E. Pasero, and S. Navaretti, "Vital-ecg: A portable wearable hospital," in *2018 IEEE Sensors Applications Symposium (SAS)*. IEEE, 2018, pp. 1–6.

[7] K. Sudheep and S. Joseph, "Review on securing medical big data in healthcare cloud," in *2019 5th International Conference on Advanced Computing & Communication Systems (ICACCS)*. IEEE, 2019, pp. 212–215.

[8] M. Yousefi-Azar, V. Varadharajan, L. Hamey, and U. Tupakula, "Autoencoder-based feature learning for cyber security applications," in *2017 International joint conference on neural networks (IJCNN)*. IEEE, 2017, pp. 3854–3861.

[9] T. Tamura, "Current progress of photoplethysmography and spo2 for health monitoring," *Biomedical engineering letters*, vol. 9, no. 1, pp. 21–36, 2019.

[10] K. Matsumura, P. Rolfe, S. Toda, and T. Yamakoshi, "Cuffless blood pressure estimation using only a smartphone," *Scientific reports*, vol. 8, no. 1, pp. 1–9, 2018.

[11] M. Kachuee, M. M. Kiani, H. Mohammadzade, and M. Shabany, "Cuffless blood pressure estimation algorithms for continuous healthcare monitoring," *IEEE Transactions on Biomedical Engineering*, vol. 64, no. 4, pp. 859–869, 2016.

[12] J. Vourvoulakis and L. Bilalis, "Real-time pulse oximetry extraction using a lightweight algorithm and a task pipeline scheme," in *2021 10th International Conference on Modern Circuits and Systems Technologies (MOCAST)*. IEEE, 2021, pp. 1–5.

[13] J. Lázaro, E. Gil, R. Bailón, A. Mincholé, and P. Laguna, "Deriving respiration from photoplethysmographic pulse width," *Medical & biological engineering & computing*, vol. 51, no. 1, pp. 233–242, 2013.

[14] A. L. Goldberger, L. A. Amaral, L. Glass, J. M. Hausdorff, P. C. Ivanov, R. G. Mark, J. E. Mietus, G. B. Moody, C.-K. Peng, and H. E. Stanley, "Physiobank, physiotoolkit, and physionet: components of a new research resource for complex physiologic signals," *circulation*, vol. 101, no. 23, pp. e215–e220, 2000.